A Numerical Investigation of the Annual Variability in the Gulf of California

E. BEIER

Centro de Investigación Científica y de Educación Superior de Ensenada, Ensenada, México

(Manuscript received 11 September 1995, in final form 31 July 1996)

ABSTRACT

The observations of sea level at the annual frequency in the Gulf of California are reproduced both in amplitude and phase with a horizontal two-dimensional linear two-layer model. The main forcing agents through which variability is explained are wind stress and the action of the Pacific Ocean, which excites an internal wave in the mouth of the gulf. The surface heating is shown to play a secondary role. The response of the basin is qualitatively similar to that observed, that is, an energetic circulation in the upper layer (cyclonic in summer and anticyclonic in winter) compared to a weaker and opposite circulation in the bottom layer, as well as a transversely averaged horizontal heat flux equal both in amplitude and phase to that calculated with historical hydrographic data. The results of the simulation show that variability across the gulf is as important as the longitudinal variability.

1. Introduction

This work is closely connected to two prior papers on seasonal variability in the Gulf of California: Ripa (1990) and Ripa (1997), hereafter R90 and R97, respectively. R90 worked with sea level and atmospheric pressure data taken along the coast of the gulf, and included in his analysis both the annual and semiannual frequencies. R90 estimated an average surface velocity representative of the whole gulf that coincides in phase with, and has an amplitude smaller than the average surface velocity calculated by Ripa and Marinone (1989) in the Guaymas Basin using historical hydrographic data. The correlation of this mean velocity with the seasonal variability of the subsurface pressure was indicative of a baroclinic structure. Thus, R90 calculated that for such baroclinic structure the corresponding phase speeds are $1.6 \pm .1$ m s^{-1} for the annual signal and $1.6 \pm .3$ m s^{-1} for the semiannual signal. Using a one-dimensional two-layer model without topography, R90 indicated that the changes in sea level could be attributed mainly to the action of the Pacific Ocean in the mouth of the gulf, while the wind stress could produce a slope on the sea level along the gulf.

However, the most significant point in R90 in the context of this work is the hypothesis that the forcing in the mouth of the gulf causes a standing internal wave, dampened by the effect of friction against the bottom. Ripa (1997) suggests that the internal wave forced by the Pacific Ocean could be an incoming Kelvin wave. Kelvin-like signals were also used by Merrifield and Winant (1989) and Merrifield (1992) to explain the mesoscale variability in the Gulf of California.

The Kelvin wave scenario, as called by R97, is backed by the observations of the sea level in the coastal stations (see Fig. 1). However, such hypothesis requires both an observational and a numerical confirmation.

The hypothesis of a baroclinic forcing in the mouth of the gulf by the action of the Pacific Ocean in the form of a Kelvin wave is resumed in this work. Our main objective is to determine which part of the variability observed in the annual scale can be explained using a two-dimensional numerical two-layer model. In the absence of dissipation, the radius of deformation corresponding to the values of phase speed mentioned above is approximately 30 km, which is smaller than the average width of the gulf (150 km) and might then indicate a very important variability across to the gulf.

Ripa (1997) worked with sea level elevations and historical hydrographic data and showed that the sea level elevations in the gulf at the annual frequency are well correlated with the heat content in the water column, and noticed that this could occur in a layer model even without temperature change since thickness is proportional to heat content. The geostrophic surface velocities calculated from the difference of the sea level elevation on both coasts are well correlated with the horizontal heat flux. The proportionality coefficients between surface elevation and heat content, and between surface velocity and horizontal heat flux are those that correspond to the first baroclinic mode. Using a one-

Corresponding author address: Dr. Emilio Beier, CICESE, Oceanografía Fisíca, Km. 107 Carretera Tijuana-Ensenada, (22800) Ensenada, BC, Mexico.
E-mail: ebeier@cicese.mx

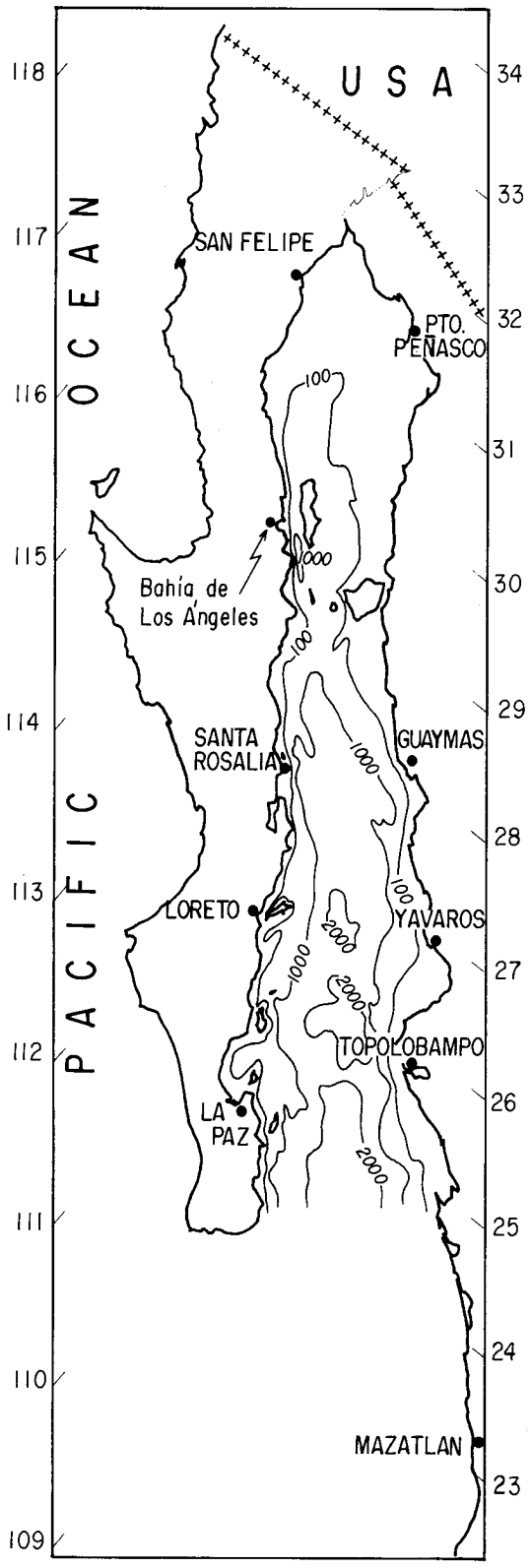

FIG. 1. The Gulf of California. Dots indicate sea level data stations.

dimensional model (transversely averaged) with topography, R97 reproduced the observations of sea level, heat content, surface velocity along the gulf, and horizontal heat flux in the annual scale and concluded that the movement and thermodynamics in this scale are mainly controlled by the Pacific Ocean, which forces an internal wave in the mouth, while the wind stress produces a slope on the sea level along the gulf. R97 also included surface heat flux as a forcing agent and concluded that its effects are minor on surface velocity and on horizontal heat flux, though not so on local heat content.

Castro et al. (1994, henceforth CLR94) estimated the annual heat balance in the Gulf of California using a historical hydrographic data bank. They calculated the heat content in the first 400 m and the heat flux through the surface for a set of boxes aligned along the gulf. Then, they estimated the horizontal heat flux needed between boxes to balance the variation of heat content and the heat through the surface. CLR94 showed that the balance of heat in the annual scale in the gulf is mainly dominated by horizontal heat transport. Ripa (1997) described the balance in the annual period as follows. The amplitude of heat input through the mouth is of 40×10^{12} *W*, and the maximum occurs on 18 May; the amplitude of the flux through the surface is of 20×10^{12} *W*, and the maximum occurs on 10 June. Together, they produce an annual heating of 59×10^{12} *W* for all the gulf, with a maximum on 26 May. The importance of the horizontal heat flux in the annual balance has already been pointed by Bray (1988) and Ripa and Marinone (1989), and an estimation like that of CLR94 is significant to the present work because in the annual scale any forcing agent in the mouth of the gulf must produce a horizontal heat flux compatible with the value that results from the hydrographic historical data.

In the present work, we assume that the baroclinic forcing in the mouth of the gulf occurs in the form of an internal wave with the transverse structure of a Kelvin wave of annual period. When it comes into the gulf, this wave will be shown to be trapped against the continental coast and then modified by topographic effects and damped by the effects of friction against the bottom. After reaching the head of the gulf, it returns as an internal wave trapped to the peninsular coast. Thus, the dynamics across the gulf can be mainly expressed in terms of an internal wave, which travels in opposite directions and is trapped to opposite walls. Our main objective is to determine whether the wind stress, the baroclinic forcing in the mouth, and surface heating, as forcing agents, can reproduce the annual variability observed on the surface of the sea, not only in spatial distribution but also in magnitude.

Bray (1988) calculated the geostrophic velocity field in four sections transverse to the gulf, from the Guaymas–Santa Rosalía transect, in the middle of the gulf, to near the head. To find the velocity field in an annual cycle, she used historical hydrographic data. Although

her results are limited by the availability of data, Bray (1988) could observe an energetic surface layer with strong transverse gradients. The circulation pattern was cyclonic in summer, with an incoming velocity on the continental side and an outgoing velocity on the Baja California side. In spring and autumn the pattern was anticyclonic.

Present research

This work deals with the dynamics of the Gulf of California on an annual scale using a two-dimensional linear two-layer model including the effects of topography, bottom friction, and lateral diffusion. The equations of the model are written using β-plane geometry. One of the effects of using a β-plane is that it permits the existence of planetary Rossby waves, although these waves are a priori expected to play an insignificant role in the dynamics under study since the topographic gradients across the gulf are more important than the variation of f. However, Rossby waves might become of some importance as they are no longer trapped against the coast. The use of the dispersion relation of long Rossby waves $\omega = -\beta k a^2$, where $a = 30$ km is the radius of deformation and ω the annual frequency, results in a value for the zonal wavelength $2\pi k^{-1} = 650$ km. Consequently, long Rossby waves with meridional wavenumber equal to zero do not fit in the gulf, which has an average width of 150 km. On the other hand, short Rossby waves could be expected to be quickly damped by dissipation. Notwithstanding, as it has not been possible to safely ignore all Rossby waves from scaling arguments, the β effect has been included and compared to the solution with an f-plane model.

The model is made linear for simplicity and in order to enable the study of each forcing in isolation so as to observe the effect each one produces in the total circulation. The values used for wind stress are those estimated by R90, and those for the heat flux through the surface are the ones calculated by CLR94. These two forcing agents are the result of meteorological observations in the gulf, at the annual frequency. There are no direct observations of the baroclinic forcing in the mouth of the gulf at the annual frequency as would result from measuring the density field in the scale considered in this work. Therefore, the baroclinic forcing that produces the horizontal heat flux estimated by CLR94 from historical hydrographic data was used instead.

2. The ocean model

a. Equations of motion

The model is a linear version of a model of inhomogeneous layers in primitive equations (ILPE). Both the description and conservation laws for this model can be found in Ripa (1993), so only a brief discussion of the equations is provided here. The model consists of two active layers of fluid on top of a rigid bottom corresponding to $z = h_0(x,y)$. The upper and bottom layers have an instantaneous layer thickness (h_1, h_2) with (H_1,H_2) as their mean value (see Fig. 2).

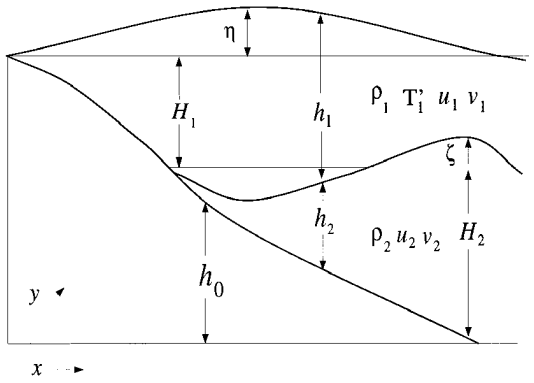

FIG. 2. Two-layer model with topography.

Coordinate x extends along the gulf and increases toward the mouth; $x = 0$ is the head of the gulf. Coordinate y extends across the gulf and increases from Baja California toward Mexico's mainland. If ρ_1 and ρ_2 are the densities in each layer, the buoyancies are defined by

$$\theta_i = g\frac{\rho_i}{\rho_0}, \tag{1}$$

where the subscript i is a layer index ($i = 1,2$), g is the gravity, and ρ_0 is a constant density used in the Boussinesq approximation. The buoyancy for each layer is expressed as

$$\theta_1(x, y, t) = \tilde{\theta}_1 + \theta'(x, y, t) = g\frac{\tilde{\rho}_1}{\rho_0} + g\frac{\rho_1'(x, y, t)}{\rho_0}, \tag{2}$$

$$\theta_2 = \tilde{\theta}_2 = g\frac{\tilde{\rho}_2}{\rho_0},$$

where $\tilde{\theta}_1$ and $\tilde{\theta}_2$ are constant buoyancies, with no space–time dependence, which correspond to the formulation of a model of homogeneous layers. Inhomogeneities are included only in the surface layer by means of $\rho'_1(x, y, t)$, for which the corresponding buoyancy fluctuation is $\theta'_1(x, y, t)$. Using a linear equation of state for seawater as a function of temperature only and a reference density $\rho_0(T_0)$, it is possible to relate the density of each layer to the temperature:

$$\rho_1(x, y, t) = \tilde{\rho}_1 + \rho_1'(x, y, t) = \rho_0[1 - \alpha(\tilde{T}_1 - T_0) - \alpha T_1'(x, y, t)],$$

$$\rho_2 = \tilde{\rho}_2 = \rho_0[1 - \alpha(\tilde{T}_2 - T_0)], \tag{3}$$

where α is the coefficient of thermal expansion, $\tilde{T}_1$, $\tilde{T}_2$ are constant temperatures, and $T'_1(x, y, t)$ is the temperature perturbation in the upper layer.

TABLE 1. Parameters used in the main run.

Mean thickness of upper layer	H_1	70	m
Coefficient of linear friction	λ	8×10^{-4}	m s^{-1}
Density of upper layer	$\tilde{\rho}_1$	1020	kg m^{-3}
Density of lower layer	$\tilde{\rho}_2$	1024	kg m^{-3}
Horizontal eddy viscosity	μ	30	m s^{-1}
Coefficient of thermal expansion	α	2.4×10^{-4}	K^{-1}
Heat capacity of water at constant pressure	c_p	4.0×10^{3}	J kg^{-1} K^{-1}
Coriolis parameter	f_0	7.51×10^{-5}	s^{-1}
Beta parameter along x axis	β_1	-1.71×10^{-11}	m^{-1} s^{-1}
Beta parameter along y axis	β_2	0.961×10^{-11}	m^{-1} s^{-1}

The momentum equations for the upper layer are

$$\frac{\partial u_1}{\partial t} - f(x, y)v_1 + \left\langle \frac{\partial p_1}{\partial x} \right\rangle = \mu \nabla^2 u_1 + \frac{\tau^x}{H_1 \rho_0}$$

$$\frac{\partial v_1}{\partial t} + f(x, y)u_1 + \left\langle \frac{\partial p_1}{\partial y} \right\rangle = \mu \nabla^2 v_1 + \frac{\tau^y}{H_1 \rho_0}, \quad (4)$$

where (u_1, v_1) is the velocity of the fluid and $f(x, y) = f_0 + \beta_1 x + \beta_2 y$ is the Coriolis parameter. Positive direction of the x axis is along 155° clockwise from the north, μ is the horizontal eddy viscosity coefficient, and (τ^x, τ^y) is the wind stress. Values of β_1 and β_2 are shown in Table 1. Thermodynamics are included in the model enabling ρ_1 to vary in space and time, which can be done in a layered model if a vertical average of the pressure force gradient is calculated inside each layer when computing the horizontal acceleration. These averages are

$$\left\langle \frac{\partial p_1}{\partial x} \right\rangle = \tilde{\theta}_1 \frac{\partial}{\partial x}(h_0 + h_1 + h_2) - \frac{H_1}{2} g\alpha \frac{\partial T_1'}{\partial x}$$

$$\left\langle \frac{\partial p_1}{\partial y} \right\rangle = \tilde{\theta}_1 \frac{\partial}{\partial y}(h_0 + h_1 + h_2) - \frac{H_1}{2} g\alpha \frac{\partial T_1'}{\partial y}. \quad (5)$$

The continuity equation for the upper layer is

$$\frac{\partial h_1}{\partial t} + \frac{\partial}{\partial x}(H_1 u_1) + \frac{\partial}{\partial y}(H_1 v_1) = 0, \quad (6)$$

and the heat equation is

$$\frac{\partial T_1'}{\partial t} = \frac{Q_s}{\tilde{\rho}_1 c_p H_1}, \quad (7)$$

where Q_s is the surface heat flux, and c_p is the heat capacity of water at constant pressure.

The momentum equations for the bottom layer are

$$\frac{\partial u_2}{\partial t} - f(x, y)v_2 + \left\langle \frac{\partial p_2}{\partial x} \right\rangle = \mu \Delta^2 u_2 - \frac{\lambda}{H_2} u_2$$

$$\frac{\partial v_2}{\partial t} + f(x, y)u_2 + \left\langle \frac{\partial p_2}{\partial y} \right\rangle = \mu \Delta^2 v_2 - \frac{\lambda}{H_2} v_2, \quad (8)$$

where (u_2, v_2) is the velocity of the fluid, and λ is the bottom friction coefficient. The horizontal gradient of pressure in the bottom layer averaged within the layer is found to be

$$\left\langle \frac{\partial p_2}{\partial x} \right\rangle = \tilde{\theta}_2 \frac{\partial}{\partial x}(h_0 + h_2) + \tilde{\theta}_1 \frac{\partial h_1}{\partial x} - H_1 g\alpha \frac{\partial T_1'}{\partial x}$$

$$\left\langle \frac{\partial p_2}{\partial y} \right\rangle = \tilde{\theta}_2 \frac{\partial}{\partial y}(h_0 + h_2) + \tilde{\theta}_1 \frac{\partial h_1}{\partial y} - H_1 g\alpha \frac{\partial T_1'}{\partial y}, \quad (9)$$

and the continuity equation for the lower layer is

$$\frac{\partial h_2}{\partial t} + \frac{\partial}{\partial x}(H_2 u_2) + \frac{\partial}{\partial y}(H_2 v_2) = 0. \quad (10)$$

Surface elevation $\eta(x, y, t)$ and the interface displacement $\zeta(x, y, t)$ are expressed as

$$\eta = h_1 + h_2 - H_T \quad (11)$$

$$\zeta = h_2 - H_2, \quad (12)$$

where $H_T = H_1 + H_2$.

b. Open boundary conditions

In the absence of topography ($H_2 = \text{const}$), it is possible to search for solutions with a proportionality between transport ($H_1 u_1$, $H_1 v_1$ for the top layer and $H_2 u_2$, $H_2 v_2$ for the bottom layer) and heights (h_1 for upper layer and h_2 for lower layer); namely,

$$H_2 u_2 = -\gamma H_1 u_1 \qquad H_2 v_2 = -\gamma H_1 v_1$$

$$h_2 - H_2 = -\gamma(h_1 - H_1). \quad (13)$$

Assuming that

$$\epsilon = \frac{\rho_2 - \rho_1}{\rho_2} \quad (14)$$

is small, the proportionality coefficient becomes

$$\gamma = 1 - \epsilon \frac{H_2}{H_T} + O(\epsilon^2) \quad (15)$$

for the baroclinic or internal mode (no mean flow at the leading order in ϵ), and

$$\gamma = -\frac{H_2}{H_1} + \epsilon \frac{H_2}{H_T} + O(\epsilon^2) \quad (16)$$

for the barotropic or external one (no vertical shear flow at the leading order in ϵ). This is a typical solution to decomposing a system of equations (4), (6), (8), and (10) into two orthogonal oscillation modes, which at the leading order in ϵ are related with the velocity and pressure field as

$$U = \frac{H_1u_1 + H_2u_2}{H_T}, \qquad V = \frac{H_1v_1 + H_2v_2}{H_T},$$
$$u = u_1 - u_2, \qquad v = v_1 - v_2,$$
$$P = \frac{H_1p_1 + H_2p_2}{H_T}, \qquad p = p_1 - p_2, \tag{17}$$

where (U, V) is the velocity of the barotropic mode, (u, v) is the velocity of the baroclinic mode, and (P, p) the barotropic and baroclinic pressure, respectively. If topography is considered, such decomposition is still possible but the spatial variability of $H_2(x, y)$ implies that modes are dynamically coupled.

In order to study the annual variability, we have used the forcing agents that excite mainly the baroclinic mode. The internal Kelvin wave forced in the mouth is baroclinic. Wind stress affects the baroclinic mode more than it affects the barotropic mode; it produces an important barotropic signal only in coastal regions, and even then the offshore barotropic transport is almost null. If the barotropic forcing is not present, the question is whether topographic variations, which in the Gulf of California are important, can generate a barotropic signal as a result of topographic coupling.

The conditions under which the baroclinic movement can remain isolated if topography is present were studied by Cushman-Roisin and O'Brien (1983), who estimated that, if the baroclinic movement is characterized by an angular frequency ω and a wavenumber k and the conditions

$$\omega^2 \ll gH_Tk^2$$
$$\omega f \ll gH_Tk^2$$
$$\frac{|\nabla H_2|}{H_2} \ll k \tag{18}$$

are met, the baroclinic movement is not altered by the topography variation; that is, the baroclinic movement is modulated only by the bottom topography with a varying internal phase speed

$$c_i^2 = g\epsilon\frac{H_1H_2}{H_T}. \tag{19}$$

The first and second conditions of Eqs. (18) are true for all the gulf at the annual scale, but the last condition is not. The topographic variations are slight only in a region near the mouth, so it is in this region where we can expect a very low degree of coupling between modes.

A no-flux normal condition in the solid walls of the model, and an open boundary condition in the mouth of the gulf located in the southernmost end have been used. The open boundary condition has been formulated assuming that in the mouth of the gulf the variables can be split into two orthogonal modes of oscillation, a barotropic one (external) and a baroclinic one (internal).

It is then postulated that each mode is the solution to the wave equation in $x = x_B$, where the mouth of the gulf is located; that is,

$$U(y, t) - \frac{P(y, t)}{c_e} = F_{\mathrm{BT}}(y, t) \tag{20}$$

$$u(y, t) - \frac{p(y, t)}{c_i} = F_{\mathrm{BC}}(y, t), \tag{21}$$

where F_{BT} represents a barotropic flux and (U, P, c_e) the normal velocity in the mouth, the pressure, and the phase speed for the external mode respectively; F_{BC} represents a baroclinic flux and (u, p, c_i) the normal velocity, the pressure, and the phase speed in the mouth of the gulf for the internal mode respectively. Similar boundary conditions were used by Bennett and McIntosh (1982). The equations for c_e and c_i are

$$c_e = \sqrt{gH_T(y)}, \qquad c_i = \sqrt{g\epsilon\frac{H_1H_2(y)}{H_T(y)}}.$$

Using (20), (21), and the relations among the variables of the model and the internal and external mode of oscillation, the instantaneous velocities for each layer are specified in $x = x_B$ as follows:

$$u_1(y, t) = U(y, t) + \frac{H_2(y)}{H_T(y)}u(y, t) \tag{22}$$

$$u_2(y, t) = U(y, t) - \frac{H_1}{H_T(y)}u(y, t). \tag{23}$$

In order to force only an incoming baroclinic wave in the mouth F_{BT} is set up to zero and

$$F_{\mathrm{BC}} = u_0\exp\left[-\frac{f(x_B, y)}{c_i}(y_{\max} - y)\right]\cos(\omega t - \Phi), \tag{24}$$

where ω is equal to one cycle per year (1 cpy $\approx 2.0 \times 10^{-7}$ s^{-1}), $y_{\max}$ corresponds to the mainland coast, and the phase Φ and u_0 are constants whose value are determined below. Equations (20) and (21) are exact for gravity waves. Their validity in this work is justified by the results of the simulation themselves.

c. Horizontal heat flux

The horizontal heat flux has to be calculated in terms of the variables of the model. The calculation in CLR94 corresponds to a balance equation of the rate of change of the stored heat, the horizontal heat flux, and the surface heat flux, all expressed as functions of coordinate x along the gulf. The heat balance estimated by CLR94 is important in the context of the dynamics proposed in

this work not only to calculate the value of the baroclinic forcing in the mouth of the gulf and the surface heat flux, but also to observe whether the spatial distribution of the horizontal heat flux obtained by CLR94 is compatible with the one resulting from this model.

The heat content in the water column per unit length is expressed as

$$\mathcal{H} = \int (\tilde{\rho}_1 c_p h_1 \Delta\tilde{T}_1 + \tilde{\rho}_2 c_p h_2 \Delta\tilde{T}_2 + \tilde{\rho}_1 c_p H_1 T_1') \, dy,$$

where $\Delta\tilde{T}_1 = \tilde{T}_1 - T_0$, $\Delta\tilde{T}_2 = \tilde{T}_2 - T_0$,

and its rate of change is then

$$\frac{\partial \mathcal{H}}{\partial t} = c_p \left(\tilde{\rho}_1 \Delta\tilde{T}_1 \int_W \frac{\partial h_1}{\partial t} \, dy + \tilde{\rho}_2 \Delta\tilde{T}_2 \int_W \frac{\partial h_2}{\partial t} \, dy + \tilde{\rho}_1 \int_W H_1 \frac{\partial T_1'}{\partial t} \, dy \right).$$

Considering the integration across the gulf and using Eqs. (6) and (7), where Q_s is a function of coordinate x only, and (10),

$$\frac{\partial \mathcal{H}(x, t)}{\partial t} = -\frac{\partial F(x, t)}{\partial x} + Q_s(x, t) \, W(x) \qquad (25)$$

is obtained, where

$$F(x, t) = \tilde{\rho}_1 c_p \Delta\tilde{T}_1 \int_W (H_1 u_1) \, dy + \tilde{\rho}_2 c_p \Delta\tilde{T}_2 \int_W (H_2 u_2) \, dy \qquad (26)$$

is the horizontal heat flux and

$$W(x) = y_{\max} - y_{\min} \qquad (27)$$

is the width of the gulf. Equation (25) is the balance equation used by CLR94 now expressed in terms of the variables of the numerical model.

d. Numerical method

Solutions to the system of equations (4), (6), (7), (8), and (10) are found numerically on a staggered grid system. Variables are defined in rectangular grid boxes of dimensions Δx and Δy. The T'_1 and h_i points are located at the center of the grid boxes. The u_i and v_i points are located on the longitudinal (along the gulf) and traversal (across the gulf) edges of the boxes respectively. Equations (4), (6), (7), (8), and (10) are forward differenced in time using the leapfrog scheme except every 20 time steps, where the Euler-backward scheme is used in order to avoid time-splitting instability. All terms of the equations are evaluated at central time level except diffusive terms and friction terms, which are evaluated at the backward time level. The time step is 12 s and the grid spacing is $\Delta x = \Delta y = 6.623$ km.

e. Parameter choices

The parameters used are those shown in Table 1, unless otherwise specified. Those that describe the basic state were calculated by R97 from the analysis of hydrographic observations and of sea level using a one-dimensional two-layer model without topography.

The topography of the gulf is highly variable, reaching 3700 m in the deepest regions toward the south. In the central part of the gulf there is a series of islands and channels and the topography varies abruptly, thus dividing the gulf in two well-defined regions: a shallow one to the north and a deep one to the south.

As the real topography is used in this work, the phase speeds for the barotropic and baroclinic modes vary from one point to another. A maximum thickness of upper layer $H_1 = 70$ m was chosen, and then interior regions with two layers where $H_1 = 70$ m and a coastal region with only one layer where $H_1 < 70$ m were determined. The mean depth of the gulf is 730 m, and a mean phase speed 1.60 m s^{-1} is required. Then, $\Delta\rho = 4$ kg m^{-3}, which represents a difference of mean temperature between layers of 17 K.

A coefficient of linear friction $\lambda = 8 \times 10^{-4}$ m s^{-1} has been included, which divided by the mean depth of the gulf is equal to the inverse of 10 days. The value chosen for λ is only tentative and cannot be strongly justified.

3. Solutions

a. Wind stress experiment

The wind is partly responsible for the variability under study. The value chosen for τ/ρ is that calculated by R90, who estimated, at the annual frequency, an amplitude of 3.8×10^{-5} m^2 s^{-2} for the longitudinal component of the wind stress (along the gulf) and a phase corresponding to a maximum in February. Thus, the wind on the gulf changes direction with the season, blowing to the NW in summer and to SE in winter. These values for wind stress result from estimating the geostrophic wind calculated from the difference of atmospheric pressure at sea level between Guaymas and Santa Rosalía (see Fig. 1), located on each coast approximately in the middle of the gulf.

For this numerical experiment, all the other forcing

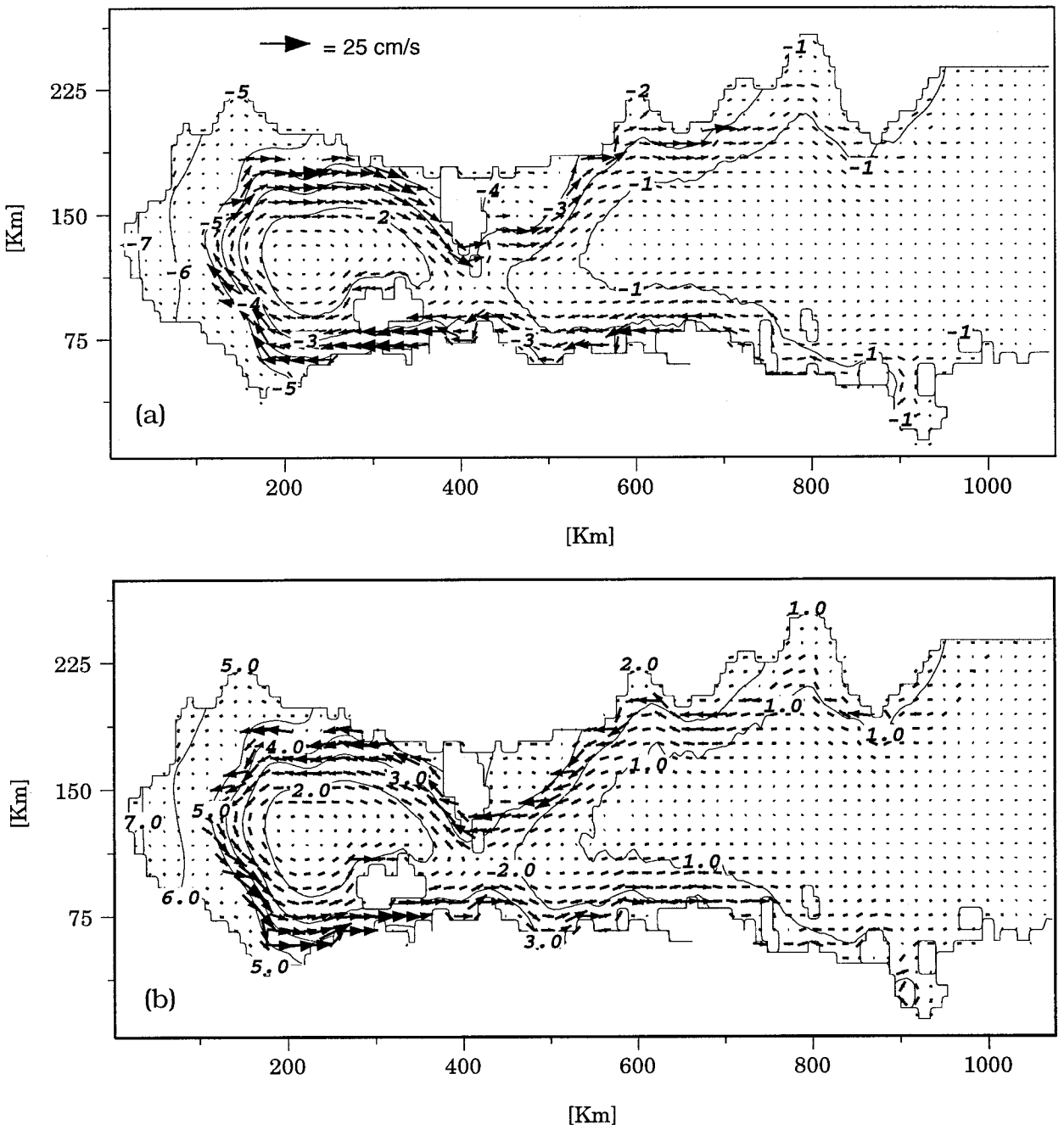

FIG. 3. Wind stress experiment. (a) Upper-layer currents and sea surface elevation (solid lines) in centimeters for (a) winter (February) and (b) summer (August).

agents as well as horizontal diffusion have been kept equal to zero so as to evaluate the effect of wind stress in isolation. The run was carried out using *f*-plane dynamics. After integrating 7 years, a state of equilibrium is reached in which the total energy cycle does not change from one year to the other. The resulting fields are shown in Fig. 3.

Figure 3a shows the velocities of the upper layer and the free surface elevations for a typical winter situation (February), when the maximum surface depressions occur. Circulation is anticyclonic in the whole gulf, with maximum velocities of 25 cm s^{-1} in the north. These are restricted to the interior region and decrease substantially in a deformation radius toward the center. In the regions where there is only one layer, velocities are very low, on the order of 3 cm s^{-1}, which indicates the baroclinic behavior of the circulation produced by the wind in all the gulf. The depressions of sea level increase

toward the head of the gulf with considerable transverse variability.

The opposite situation is shown in Fig. 3b, which corresponds to summer (August). The circulation pattern is cyclonic and there is an important cyclonic gyre in the northern gulf region, between the head and the area of the big islands. It is noteworthy that although the wind stress does not have a structure transverse to the gulf, the circulation pattern produced by the wind shows a very important variability across the gulf.

From now on, amplitudes and phases of any variable, whether observed or calculated by the model, are those that result from least square fitting to a curve of the form

$$S(t) = S_0 \cos(\omega t - \Phi),$$

where ω is the annual frequency. Thus, the variable $S(t)$ at any point (x, y) is represented by its amplitude and phase (S_0, Φ). In order to study the behavior of the fields obtained along the gulf, a transverse average was calculated with

$$\bar{\xi}(x, t) = \frac{1}{W(x)} \int_{y_{\min}}^{y_{\max}} \xi(x, y, t)\, dy \tag{28}$$

so that $\bar{\xi}(x, t)$ represents the transverse mean value of a variable in the model. These variables were calculated by R97 using a one-dimensional model transversely averaged, in spite of the width of the gulf being larger than the internal deformation radius. Thus, it was not clear a priori whether or not the across-gulf average of the results of this paper would coincide with those of R97. The agreement is, in fact, not perfect, thereby partly confirming the approximations of Ripa's model and partly showing its limitations.

The important longitudinal and transverse variability can be explained with some simplifications and using the results of the simulation itself. That is, the response to the wind is mainly located on both coasts of the gulf and decreases with the radius of deformation, which is small if compared to the width of the gulf, and the circulation pattern is markedly baroclinic. Assuming that conditions (18) were true in the gulf—that is, in spite of topography variations the baroclinic movement is not altered and is modulated only by bottom topography, the equations of the baroclinic movement in terms of the variables of the upper layer can then be expressed, if $\lambda = \mu = 0$, as

$$\frac{\partial u_1}{\partial t} - f v_1 = -\frac{c^2}{H_1}\frac{\partial h_1}{\partial x} + \frac{H_2}{H_T H_1}\frac{\tau^x}{\rho_1} \tag{29}$$

$$\frac{\partial v_1}{\partial t} + f u_1 = -\frac{c^2}{H_1}\frac{\partial h_1}{\partial y} + \frac{H_2}{H_T H_1}\frac{\tau^y}{\rho_1} \tag{30}$$

$$\frac{\partial h_1}{\partial t} + \frac{\partial H_1 u_1}{\partial x} + \frac{\partial H_1 v_1}{\partial y} = 0, \tag{31}$$

where c is given by (19) and the variables for the bottom layer are

$$(H_2 u_2, H_2 v_2, h_2 - H_2) = -\gamma(H_1 u_1, H_1 v_1, h_1 - H_1), \tag{32}$$

where γ is as in (15). For the sake of simplicity, let us consider H_2 constant and two layers in the whole area, the movement along a wall aligned with the x axis, located in $y = 0$, and the wind blowing in that direction. In the model, this corresponds to the Baja California side. It is also assumed that the region is far from the head. The scale of the longitudinal movement is $L =$ 1000 km (the length of the gulf), much larger than the radius of deformation. In addition, let's consider a timescale $T = Lc^{-1}$, much larger than the timescale of f^{-1}. Similar scaling arguments were used by Gill (1982, pp. 398–403), to deal with a forced Kelvin wave along a straight coast. With these scaling arguments and simplifications, Eq. (30) is reduced to

$$u_1 = -\frac{c^2}{f H_1}\frac{\partial h_1}{\partial y} = -\frac{1}{f}\frac{\partial p_1}{\partial y}; \tag{33}$$

that is, u_1 is in geostrophic balance, and the potential vorticity equation is reduced to

$$\frac{\partial u_1}{\partial y} + f\left(\frac{h_1 - H_1}{H_1}\right) = 0. \tag{34}$$

Using the last two equations it is possible to obtain an equation for h_1, which when integrated and considering only the solution that decreases results in

$$h_1 = A(x, t)\exp\left(-\frac{y}{a}\right) + H_1 \tag{35}$$

$$u_1 = \frac{c}{H_1}A(x, t)\exp\left(-\frac{y}{a}\right), \tag{36}$$

where $a = cf^{-1}$ is the deformation radius. The response generated in the opposite wall rapidly decreases with a and therefore can be neglected near $y = 0$; this has the form

$$h_1 = B(x, t)\exp\left(\frac{y - W}{a}\right) + H_1 \tag{37}$$

$$u_1 = -\frac{c}{H_1}B(x, t)\exp\left(\frac{y - W}{a}\right). \tag{38}$$

Equations (35)–(38) indicate that the fields have a trapping length of 30 km on both sides of the walls and, then, do not overlap because the width of the gulf is 150 km.

Figures 4 and 5 correspond to the instantaneous fields of the Guaymas–Santa Rosalía section, obtained with the model for a typical summer (August) situation, when the wind blows toward the head. The behavior of the

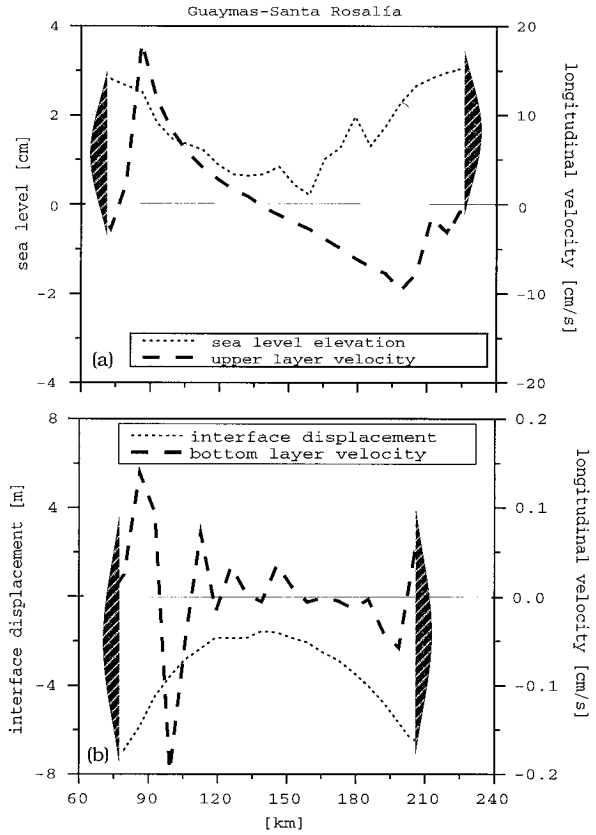

FIG. 4. Wind stress experiment. Cross section between Guaymas and Santa Rosalía. Instantaneous fields for summer (August) as a function of coordinate transverse to the gulf: (a) sea level elevation and longitudinal component of upper-layer velocity and (b) interface displacement and longitudinal component of bottom-layer velocity.

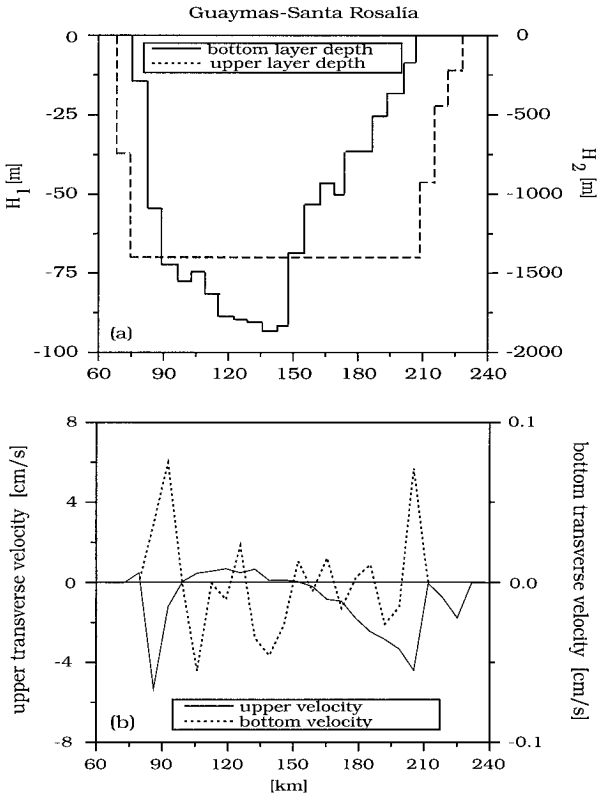

FIG. 5. Cross section between Guaymas and Santa Rosalía: (a) upper- and bottom-layer depth and (b) upper and bottom transverse velocities for summer (August) for the wind stress experiment.

variables is very similar to that estimated with (35), (36), (37), and (38); that is, sea level is proportional to $(h_1 - H_1)$, the interface displacement is proportional to $-(h_1 - H_1)$, and the upper velocity decreases toward the interior of the section with *a.* In addition, the relative phase among these variables is the one estimated with (35), (36), (37), and (38). In Fig. 4 the shadow areas indicate the walls of the gulf; the topography can be seen in Fig. 5a. On both sides of the gulf, u_1 increases rapidly up to a maximum and then decreases with *a* toward the center of the section, as can be estimated with (36) and (38). Very near the coast there is only one layer and velocities are small. Where depth enables two layers, velocities increase offshore to match the Kelvin wave solution. This confines the dynamics to the interior region. Although the movement is mainly baroclinic, near the boundaries there is a barotropic component as can be seen in Figs. 4a and 4b. The velocities of the bottom layer are much lower than those of the upper layer in agreement with relation (32) and are more irregular, as they are directly affected by topography and friction against the bottom.

More information about coefficients $A(x, t)$ and $B(x, t)$ is needed to explain longitudinal variability produced by the wind stress, so replacing (35) and (36) in (29) and (37) and (38) in (29) again and evaluating in $y = 0$ and $y = W$ respectively,

$$\frac{\partial A(x, t)}{\partial t} + c\frac{\partial A(x, t)}{\partial x} = \frac{H_2}{cH_T\rho_1}\frac{\tau}{} \quad \text{at } y = 0 \qquad (39)$$

$$\frac{\partial B(x, t)}{\partial t} - c\frac{\partial B(x, t)}{\partial x} = -\frac{H_2}{cH_T\rho_1}\frac{\tau}{} \quad \text{at } y = W, \qquad (40)$$

which correspond to two equations of waves forced by the wind and can be seen as forced Kelvin waves, each trapped against one of the walls of the gulf. Then $A(x, t)$ and $B(x, t)$ are the relevant variables of the problem since they are proportional to sea level elevations and interface displacement along the coast. Assuming a summer situation, when the wind blows toward the head, the sign of τ is negative, which means from (40), that 1) an internal wave was generated on the continental wall, the amplitude of which increases linearly from a null value in the mouth to a maximum value in the head, 2) the elevation of the sea level is positive, and 3) the velocity of the upper layer is negative (incoming). After going around the head, the wave propagates outward, trapped against the Baja California wall. Now the wind stress is in the opposite direction, as in (39), the upper-

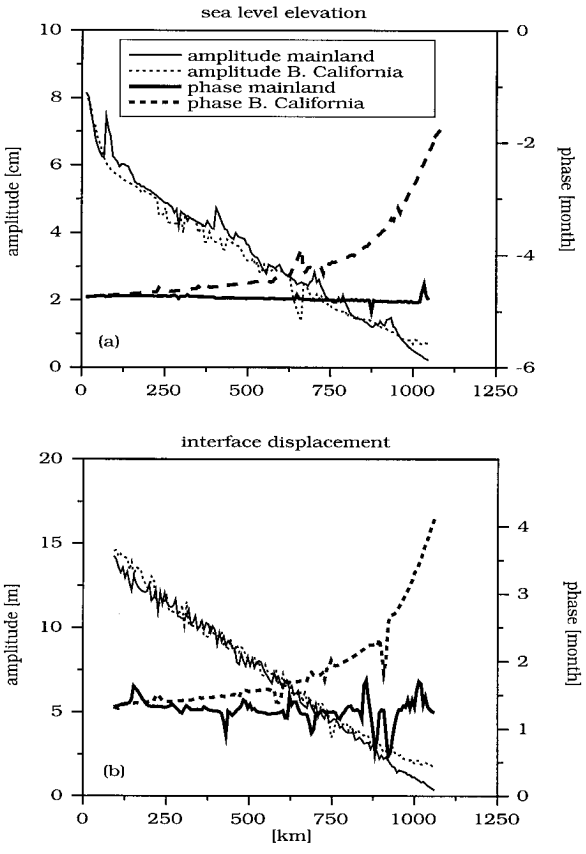

FIG. 6. Wind stress experiment: Coastal amplitudes and phases of the sea level elevation (a) and the interface displacement (b) as a function of the distance to the head of the gulf.

layer velocity is positive (outgoing), and the sea level is positive but decreases toward the head. Thus, it is now an internal wave modified by the effect of wind from a maximum value in the head to a practically null value in the mouth.

Figure 6 shows the amplitudes and phases along the coast of Baja California and the continent as a function of the distance to the head of the gulf for the sea surface elevation and the interface displacement obtained with the simulation. The amplitudes grow from a practically null value in the mouth up to a maximum value in the head. This behavior can be justified using (39) and (40). With the values from Table 1 and a global phase speed of 1.6 m s^{-1}, (39) predicts a value of 14.15 m for the interface amplitude in the head, which is very close to the value from the simulation, of 14.25 m. In Guaymas–Santa Rosalía the simulation gives values of 6.91 m on Baja California and 6.58 m on the continent, very close to the value calculated with relation (39), of 7.07 m.

Coefficient $A(x, t)$ is different from $B(x, t)$ because the internal wave propagates trapped modes against different walls and is modified by friction and topography. Although the amplitudes are similar for a fixed distance from the head, there is an important difference of phase, as can be seen in Figs. 6a and 6b. There is a difference of phase of 12 days between the Guaymas and Santa Rosalía stations for the wind-forced solution prognosticated by the model.

Transverse velocities for bottom and upper layers (Fig. 5b) are the most influenced by the topographic changes near the walls. However, in the central area of the section, the transverse velocity of the upper layer is positive and has a maximum value of 0.69 cm s^{-1}. From the continuity equation (31)

$$v_1 = \frac{\tau H_2}{\rho H_T H_1 f}\left[\exp\left(-\frac{y}{a}\right) - 1\right] \quad \text{near } y = 0 \qquad (41)$$

$$v_1 = \frac{\tau H_2}{\rho H_T H_1 f}\left[\exp\left(\frac{y - W}{a}\right) - 1\right] \quad \text{near } y = W. \qquad (42)$$

Far from both walls, the Ekman drift $v_1 = -\tau H_2/(\rho H_T H_1 f)$ is obtained. For the summer situations, τ is negative. Using the values from Table 1 and evaluating in the center of the section, a central value of 0.64 cm s^{-1} is obtained, which is very close to the results of the simulation.

Thus, the circulation pattern produced by the wind stress can be explained if it is assumed that in this scale the wind produces a forced internal wave trapped against the coast around the gulf, and all the dynamics are strongly influenced by a small radius of deformation. Circulation is then inverted from cyclonic to anticyclonic from summer to winter.

b. Baroclinic wave experiment

In order to study the variability on an annual scale, the transverse structure of a baroclinic Kelvin wave of annual period of the form (24) was forced at the mouth of the gulf. The horizontal heat flux in the mouth was estimated by CLR94, who calculated a total value of 40 TW of amplitude and a phase corresponding to a maximum in November. In the wind stress experiment, it was found that the wind causes a horizontal heat flux in the mouth of 6.7 TW (1 terawatt = 10^{12} W) of amplitude and phase corresponding to a maximum in November. These values coincide with those obtained by R97. In (24), u_0 and Φ were chosen so that the superposition of the response of the baroclinic wave and that due to wind stress match the heat flux at the mouth calculated by CLR94; that is, the incoming baroclinic wave must produce a flux of 33 TW and phase in November.

In this experiment, an incoming internal wave was used as the only forcing agent. The rest of the forcing agents (wind stress and surface heating) and the horizontal eddy viscosity μ were set to zero and the run was carried out in the f plane.

The simulation starts from a rest state. During the first days the internal wave propagates toward the interior of the gulf, trapped to the wall of mainland Mex-

ico. It is amplified by the effects of topography and dampened by the effects of friction against the bottom.

Once the baroclinic wave reaches the head, it goes around the head and out of the gulf as a baroclinic wave trapped to the Baja California coast. Thus, the dynamics are mainly expressed in terms of two internal waves that travel in opposite directions trapped against opposite walls. There is little overlapping between both waves because the internal radius of deformation is small compared to the width of the gulf. After integrating 7 years, a state of equilibrium is reached in which the total energy cycle is the same from year to year.

The fields that result from this equilibrium are shown in Fig. 7a, which illustrates the amplitudes (in cm) and phases (in days) of the free surface. The maximum amplitudes occur on the coast of the gulf where they reach 12 cm and diminish to 1.5 cm toward the center of the gulf. The amplitudes produced along the coasts of the gulf are almost constant. There is a great traversal variability due to the fact that the average internal radius of deformation is 30 km, a small value if compared to the width of the gulf, which has an average of 150 km and reaches up 210 km. The longitudinal variability of the sea surface is greater in the region of the big islands, where the gulf section diminishes considerably, and in the head, where the wave turns around.

The phases show that the maximum elevations of the free surface occur in all the gulf in August. However, there is an important lateral variability, particularly in the southern region of the gulf. The greatest traversal variability occurs in the mouth when the maximum elevations occur on the Mexican mainland coast at the beginning of August and on the Baja California side at the end of August, with a resulting difference of phase of 16 days. Considering an average phase speed of 1.6 m s^{-1} for the whole gulf and a length of the gulf equal to 1000 km, the annual Kelvin wave should have a phase difference of 15 days, a value very close to the result of the model.

Figure 7b shows the contours of amplitudes (in m) and phase (in days) for the interface. The maximum amplitudes are on the order of 30 m on the coast of the gulf and show a great lateral variability, again resulting from a small internal radius of deformation. There is a spatial distribution similar to that of the sea surface elevation, and the phase is such that both fields have opposite signs.

In summer the circulation in the upper layer is cyclonic in the whole gulf, with outgoing flow on the Baja California side. Positive elevations of the free surface correspond to the summer cyclonic flow. Taylor (1921) studied the reflection of a barotropic Kelvin wave in a semi-infinite channel. Taking a semi-infinite channel with dimensions similar to those of the gulf and the annual frequency, Taylor's solution is two Kelvin waves traveling on both sides of the channel. Near the head, evanescent Poincaré modes are required in order to satisfy no flux condition. Both Kelvin waves can be seen in (39) and (40) making $\tau = 0$, and the relative phases between h_1 and u_1 are given by (35), (36) and (37), (38), and then $v_1 = 0$ as in (41) and (42). Since h_1 and u_1 decrease with a toward the center of the channel, the two Kelvin waves do not overlap. In Taylor's solution, the isolines of constant phase and amplitudes of sea level and interface displacement are parallel to the wall except near the head where the wave turns. The baroclinic solution obtained with real topography is very similar to that of Taylor's problem, as can be seen in Figs. 7a and 7b. Although the transverse structure of an incoming Kelvin wave was forced in the mouth, the baroclinic wave is distorted by topography and bottom friction in the interior region.

Figure 8a shows the coastal amplitudes and phases of the sea level elevation as a function of the distance to the head of the gulf. Coastal amplitudes are irregular, particularly on the Baja California side, but vary little from 12.6 cm. The phases clearly show the propagation of the internal wave.

The pattern of circulation produced by the baroclinic wave is similar to that produced by the wind stress, that is, anticyclonic in winter and cyclonic in summer. Both forcing agents define an intense gyre in the northern region of the Gulf of California. Even though the pattern is similar in the southern region, the circulation produced by the baroclinic wave is more intense in all the gulf. However, in general, the two forcing agents, wind stress and baroclinic forcing, are in phase in all the gulf, which makes it difficult to determine, except with a model, to which forcing agent the observed variability is due. Figure 3 in R97 shows that the sea level signal seems to be a Kelvin wave propagating along the Pacific coast (including the Gulf of California) with important local modification (e.g., in the Gulf of Tehuantepec and California), which might be attributed to the wind. The origin of the large-scale annual sea level variation—to what extent it is forced by the large-scale winds or by solar heating—is clearly beyond the scope of this paper. However, a possible explanation of why the wind stress and the internal Kelvin wave at the mouth of the gulf are in phase in the gulf could be attempted if it is assumed that the internal wave presumably running up the Pacific coast reaches the mouth of the gulf and propagates directly into the gulf. This hypothesis is feasible because the gulf is rotationally wide and could be thought of as a continuation of the Pacific coastline. Thus, the internal wave could be in phase with the local response when entering the gulf if it is assumed that this wave is driven by the large-scale wind field.

Again, the fields have been transversely averaged as in (28) because it is necessary to see whether the horizontal distribution of the horizontal heat flux calculated with the model is similar to that estimated from hydrographic data by CLR94, as a function of x. The results are similar to those of R97 for the mean velocity of the upper layer but not so much for the sea level elevation and the interface displacement. Figure 8b shows the

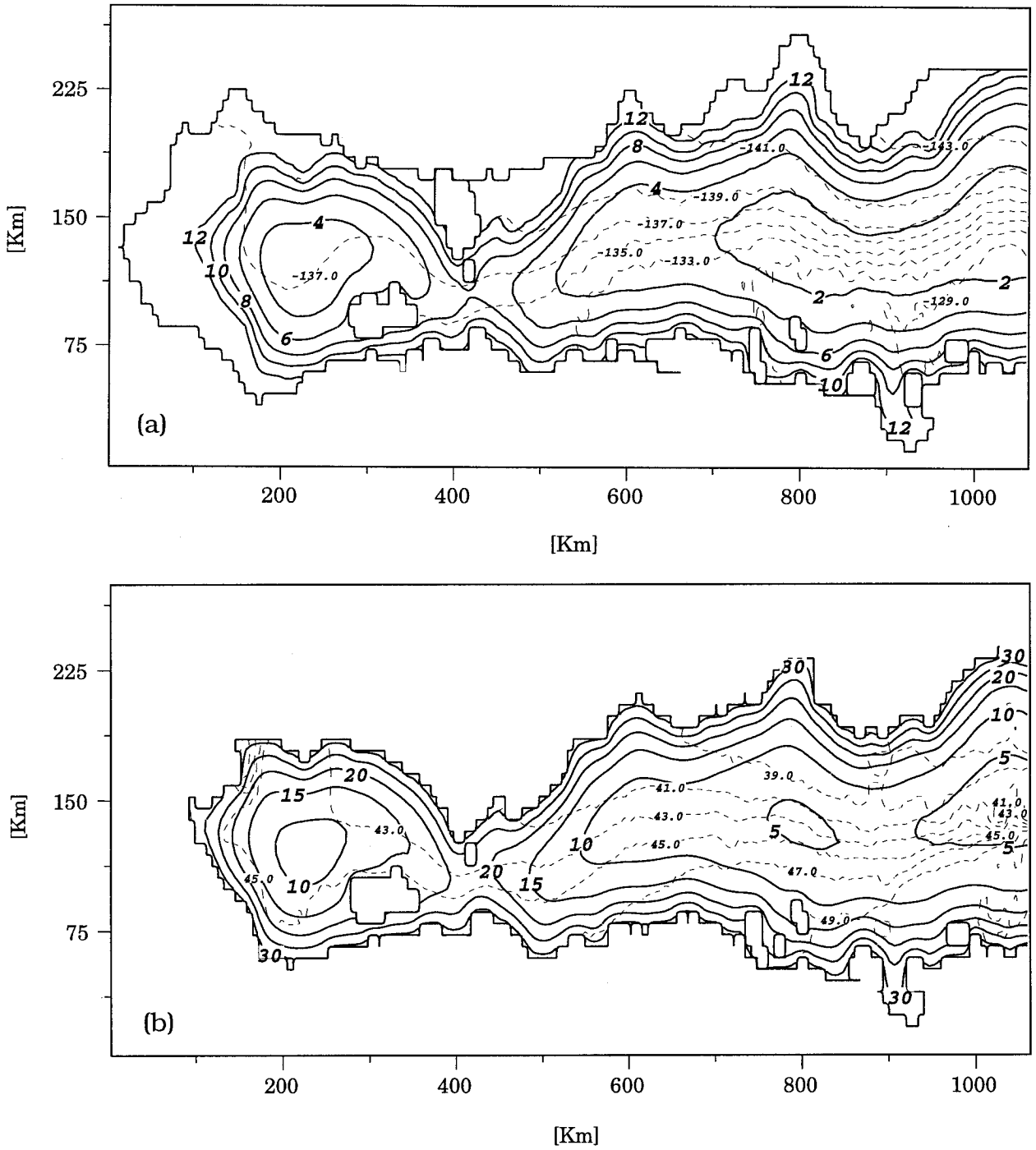

FIG. 7. Response to baroclinic wave forcing in the mouth of the gulf. (a) Contours of amplitude (solid line) in centimeters and contours of phase (dashed line) in days for the sea surface elevation. (b) Contours of amplitude (solid line) in meters and contours of phase (dashed line) in days for the interface displacement.

amplitude of the sea level elevation, which is equal to 6.30 cm in the southern part of the gulf and increases to almost 10 cm and 12.5 cm in the region of the big islands and the head of the gulf respectively. The phase is almost constant and is equal to 7.5 months (August) in the whole gulf. These two maxima in sea level elevation and in the interface displacement (not shown) are explained as follows. If the deformation radius were much greater than the width of the gulf, a decrease of the width of the section would not cause an important increase in the sea level averaged across the gulf as in the case of the semidiurnal tide. But for the case under

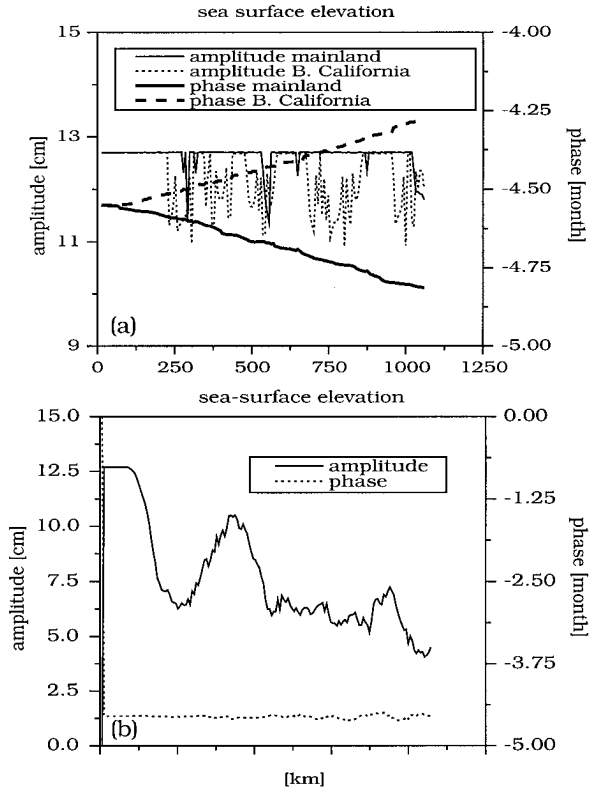

FIG. 8. Response to baroclinic wave forcing at the mouth of the gulf: (a) Coastal amplitudes and phases of the sea level elevations as a function of the distance to the head of the gulf and (b) sea level elevation average across the gulf.

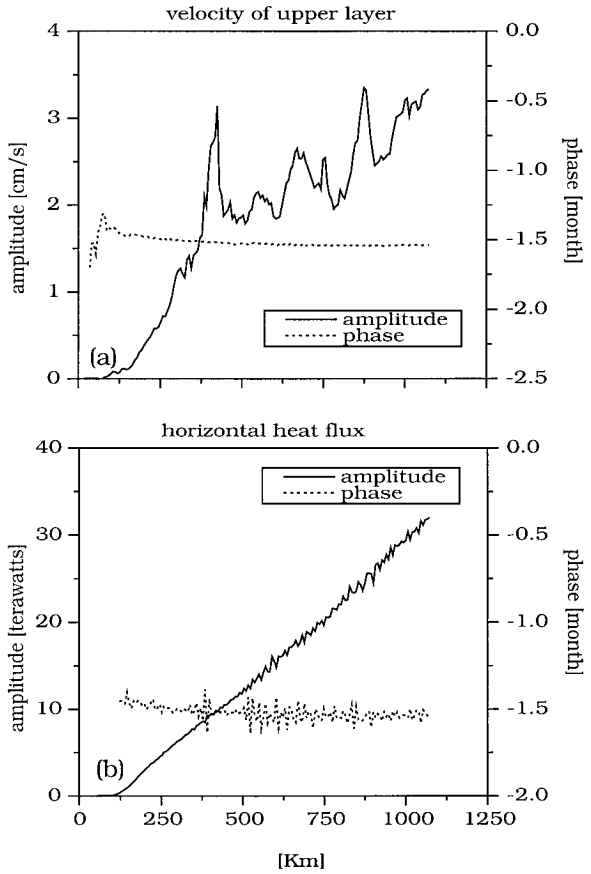

FIG. 9. Response to baroclinic wave forcing at the mouth of the gulf: (a) Upper-layer velocity and (b) horizontal heat flux averaged across the gulf as a function of the distance to the head.

study, the radius of deformation is smaller than the width of the gulf. As a result, a decrease in the transverse width up to a value on the order of a significantly alters the average, as occurs in the region of the big islands and the head. These two maxima do not appear in the one-dimensional model of R97 because f drops from the 1D equations of motion.

Each of the three variables $\bar{u}_1(x, t)$, $\bar{\eta}(x, t)$, $\bar{\zeta}(x, t)$ reaches its maximum almost at the same time in the whole gulf, and $\bar{u}_1(x, t)$, Fig. 9a, is lagged in $\pm\pi/2$ with respect to the elevation of the surface and the interface respectively, which corresponds to an internal wave, although, as shown before, this internal wave is formed by two waves traveling in opposite directions that do not overlap with each other except in isolated places.

Figure 9b corresponds to the horizontal heat flux $F(x, t)$. The amplitude decreases linearly from 32 TW in the mouth to zero in the head and the phase remains constant and equal to -1.5 months. These values are very close to those obtained by R97.

c. The main run

In this last experiment, the three main forcing agents have been included: namely, wind stress, the internal wave forced at the mouth of the gulf, and surface heat flux Q_s. The latter is included in the model by means of Eq. (7). This enables a local heating and cooling that affects the pressure gradient, though because of its linear form this contribution to heat content is not advected. The values of Q_s are those calculated by CLR94. Maximum amplitudes correspond to the central region of the gulf and reach their maxima in July.

The effect of surface heat flux on the total circulation is not important. An experiment carried out with only this forcing agent showed that it produced a horizontal heat flux with a maximum value in the mouth of 1.5 TW and a mean velocity $\bar{u}_1(x, t) = 0.15$ cm s^{-1}. The maximum variations of sea level (1.5 cm) occur in the central region.

The previous experiments were carried out in the simplest possible way. They did not include the diffusion term and f was not allowed to vary. This run includes lateral diffusion with a coefficient $\mu = 30$ m^2 s^{-1} and the simulation was carried out using β-plane dynamics. The simulation starts from a rest state, and after integrating 7 years the state of equilibrium is reached. Results can be seen in Fig. 10, which shows the upper-layer velocities and sea surface elevation for a typical

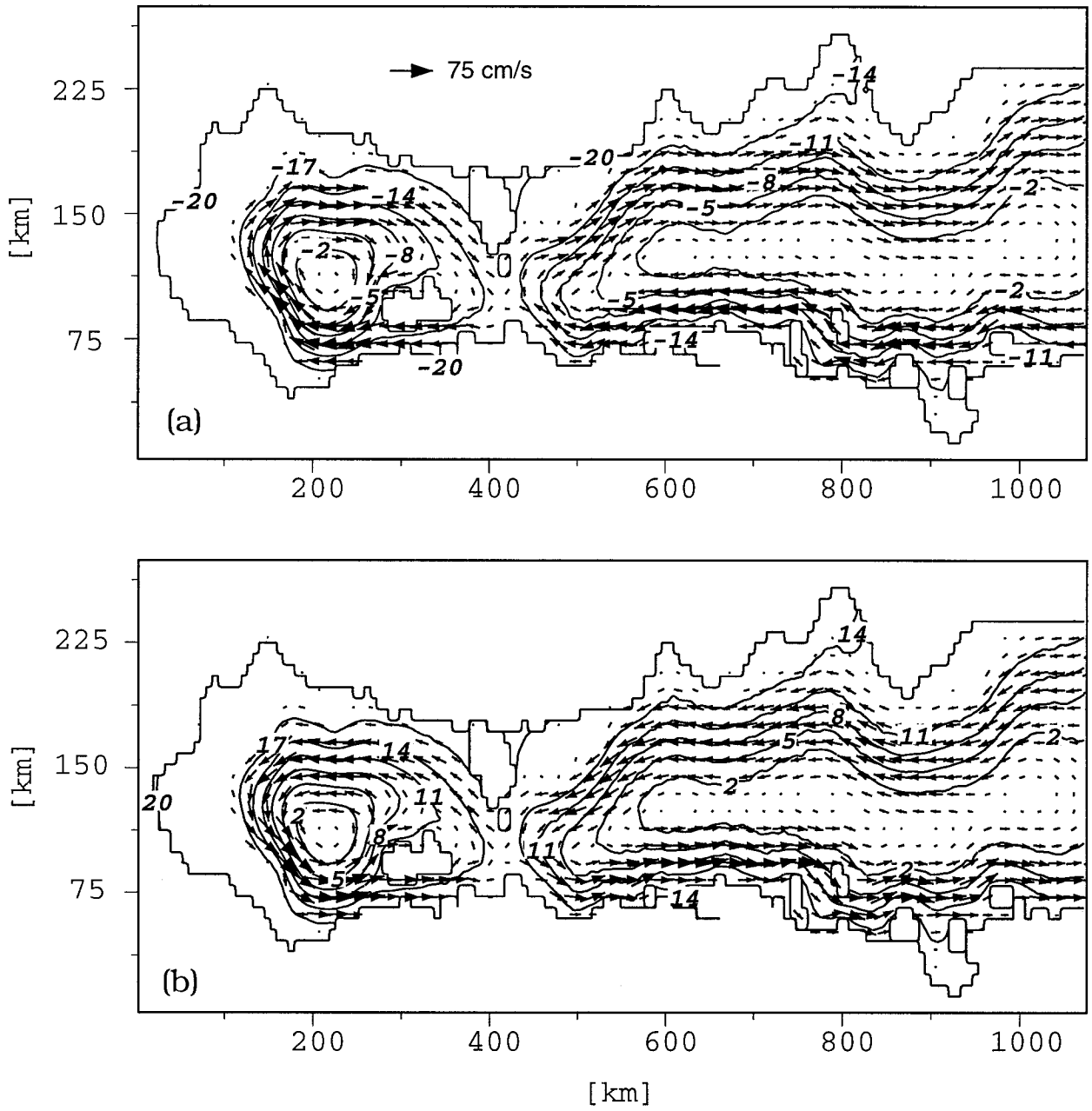

FIG. 10. The main run: Upper-layer currents and sea surface elevation in centimeters for (a) winter (February) and (b) summer (August).

winter situation (February) and summer situation (August). The pattern of circulation is similar to the superposition of the individual cases, namely, of the circulation induced by the wind stress added to the forcing of the structure of a Kelvin wave in the mouth of the gulf. The β effect exerts only a minor influence on the total circulation. The main run shows a surface anticyclonic pattern of circulation in winter and cyclonic in summer in the whole gulf but, in contrast with the previous runs, it shows two well-defined gyres. One is placed in the northern gulf and the other in the southern region. They are separated by the constriction produced by the region of big islands. The northern gyre is shifted toward the Baja California coast and situated on the Delfin Basin.

An additional run was carried out, now keeping f constant. The difference between both solutions was estimated by

$$\sigma(t) = \sqrt{\frac{\Sigma_{i,j}\,(\xi^{\beta} - \xi^{f_0})^2}{\Sigma_{i,j}\,(\xi^{\beta})^2}},$$

where ξ^{β} and ξ^{f0} are the instantaneous fields displacement for β-plane and f-plane dynamics respectively. Maximum value of $\sigma(t)$ for the sea level elevations is 1.2×10^{-4} and that of interface displacement is 2.4×10^{-2}. The longitudinal velocity of the bottom layer takes values of $\sigma = 3.3 \times 10^{-2}$, and the transverse velocity values of 2.2×10^{-2}. The maximum difference between solutions occurs in the surface velocities with values of $\sigma = 13 \times 10^{-2}$ for the longitudinal velocities and $\sigma = 7 \times 10^{-2}$ for the transverse velocities. Even though there is a difference in the upper-layer velocity, the β effect only intensifies the circulation in the upper layer but does not change the circulation pattern. The difference can be partly attributed to the fact that in the β plane the internal wave is traveling in a medium where the local internal radius of deformation varies from point to point not only with the topography but also with f.

Figure 11 shows the fields for a summer situation (August) in the Guaymas–Santa Rosalía section. The depth of each layer is as shown in Fig. 5a, and the shadow area in Fig. 11 indicates the coast of each layer. Figure 11a illustrates the sea level elevation and the velocity of the surface layer. Near the coast of Guaymas (right) it can be seen that velocities are almost null in the region where there is only one layer. In places where the topography allows two layers, the velocities (incoming) increase toward the interior of the section and then decrease with the radius of deformation near the center of the section. Thus, the dynamics are confined to the interior of the gulf. Sea level reaches a maximum value in the region where the interface intercepts the bottom and is thence transmitted toward the coast with an almost constant value. This is why the coastal region shows sea level elevations characteristic of a baroclinic movement.

The bottom layer (Fig. 11b) presents the opposite situation with outgoing velocities on the Guaymas side. Velocities show a greater variability than in the surface layers because friction and topography exert more influence there. The high values of transverse velocities in Fig. 11c are due to the fact that the section narrows in this region of the gulf.

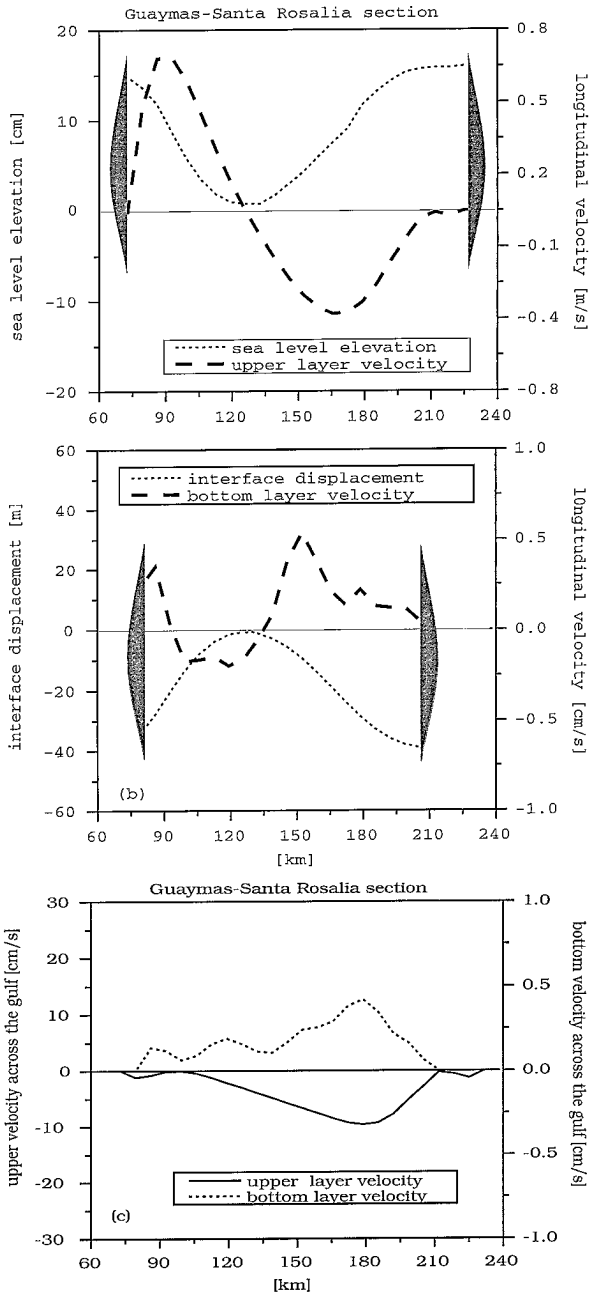

FIG. 11. The main run: Cross section between Guaymas and Santa Rosalía showing instantaneous fields for summer as a function of coordinate transverse to the gulf. (a) Sea level elevation and longitudinal upper velocity. (b) Interface displacement and longitudinal bottom velocity. (c) Upper and bottom transverse velocity.

d. Comparison with the observations

To compare the results of the simulation with the observations at the annual scale, the fields obtained with the model and corresponding to the seventh year of simulation are shown in terms of amplitude and phase. Figure 12 illustrates the horizontal heat flux transversely integrated as a function of the distance to the head. The symbols correspond to the values calculated by CLR94, and the continuous curves to the values of the model. Both values were made to coincide in the mouth; in the interior of the gulf the values calculated by the model follow a distribution similar both in amplitude and phase to those calculated by CLR94; that is, the amplitude decreases linearly toward the head and the phase remains constant and equal to 10.7 months. This result is considered important because it means that the dynamics proposed to explain the annual variability reproduces the distribution of horizontal heat flux obtained from hydrographic data.

The observations of sea level in the gulf come from eight coastal stations (see Fig. 1). The analysis of the sea level records can be found in R90 and R97, which

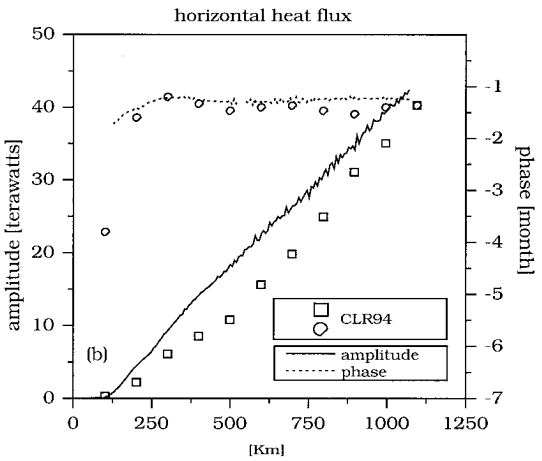

FIG. 12. The main run: Horizontal heat flux transversely averaged as a function of the distance to the head of gulf. Symbols indicate values obtained by CLR94. Solid and dotted lines are the amplitude and phase obtained with the model.

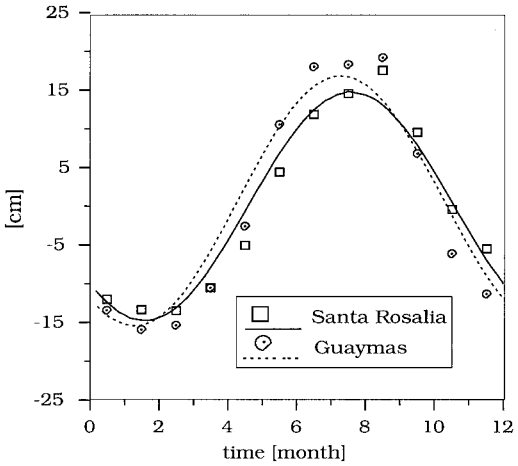

FIG. 13. Monthly means (symbols) of the sea level at two stations in the middle of the gulf and instantaneous sea level elevation obtained with the model for the last year of integration; dotted line for Guaymas and solid line for Santa Rosalía.

include a detailed description of results, length of each record, and techniques used. The analysis of sea level is absolutely robust. For example, Fig. 13 shows the monthly mean values (symbols) of two stations located opposite each other. Annual signals fitted[1] in Guaymas and Santa Rosalía (not shown) explain 96% and 98% of the variance respectively. A maximum of 19.7 cm is reached on 14 August in Guaymas and a maximum of 15.3 cm is reached on 27 August in Santa Rosalía. The differences between both stations are significant because the uncertainty of the amplitudes is of 1 cm, and that of the phases of 3 to 4 days.

In Fig. 13 the curves are the instantaneous sea level elevation obtained with the model at Guaymas (dotted line) and Santa Rosalía (solid line) in the last year of simulation. Notice that the model predicts a difference of phase between both stations similar to that observed, but it underestimates the difference of amplitude observed between the two coasts.

Table 2 shows the amplitude, phases, and percentages of the variance explained for eight coastal stations used in the present work, and the amplitudes and phases of atmospheric pressure expressed in cm of water for six stations located in the Gulf of California. In order to obtain the subsurface pressure, the sea level data were corrected by means of a linear interpolation of atmospheric pressure. The results are shown in Figs. 14a and 14b, where the amplitude and phase for each station has been plotted as a function of the distance to the head of the gulf, and coded with symbols. The bars indicate fitting errors. As can be seen in Fig. 14, the observations of sea level show a great variability both along and across the gulf. The variability longitudinal to the gulf can be seen in this figure when averaging the complex amplitudes of the observations on both coasts, which results in the amplitude increasing toward the head of the gulf and the phase remaining constant and close to 8 months. The variability traversal to the gulf shows that the amplitudes of the observations on the mainland are always larger than those on Baja California, both in the central and southern parts of the gulf.

It can be observed in Fig. 14a that the model predicts the longitudinal variability observed in the amplitudes both in the central and south part of the gulf. Near the head there are two points of observation (San Felipe and Puerto Peñasco) where the model amplitudes are larger. The results of the model also confirm the traversal variability observed; that is, the amplitudes obtained with the model on the mainland are greater than those

TABLE 2. Amplitudes, phases, and percentages of seasonal variance explained by annual harmonic.

Station	Amplitude (cm)	Phase (days)	Variance (%)
San Felipe	18.7	−140	97
Puerto Peñasco	18.1	−129	92
Bahía de los Ángeles	17.4	−131	97
Santa Rosalía	15.3	−126	98
Guaymas	19.7	−144	96
Loreto	14.5	−117	96
Yáv aros	17.1	−139	97
Topolobampo	17.0	−134	96
La Paz	12.6	−108	98
Atmospheric pressure			
San Felipe	4.6	1	91
Santa Rosalía	3.0	7	87
Guaymas	3.2	15	92
Loreto	3.4	17	93
Puerto Peñasco	4.4	12	95
Mazatlán	1.6	30	84

[1] Time series are least squares fitted to an annual harmonic using $A(t) \sim A_0 + A_1 \cos\omega t + A_2 \sin\omega t$, where $2\pi/\omega = 1$ yr and A represent the sea level elevation at a certain (x, y).

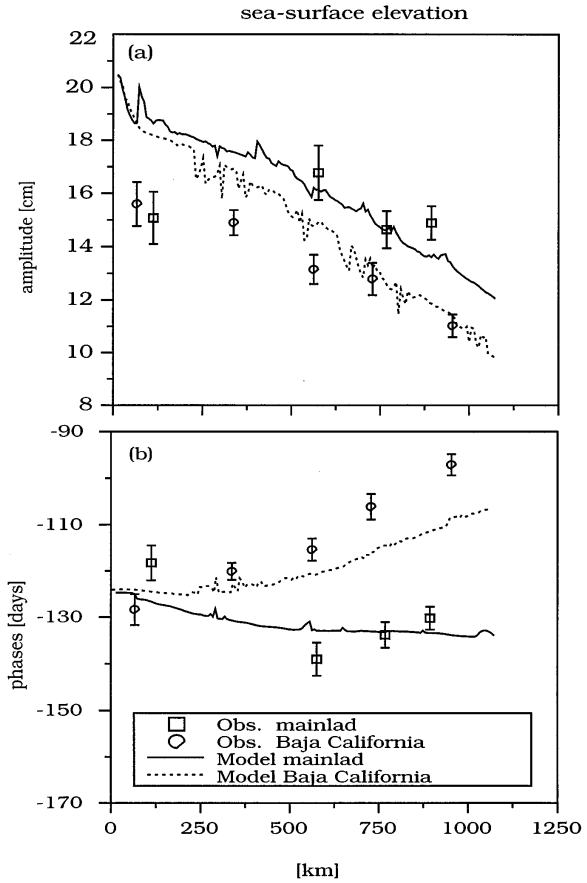

FIG. 14. The main run: Comparison between sea surface elevation obtained with the model, and observation (symbols) as a function of the distance to the head of the gulf.

obtained on the peninsula. However, the difference of amplitude between both coasts is underestimated by the model. While a maximum difference of 4 cm is observed, a maximum of only 2.3 cm is obtained with the model. In the simulation, this difference of amplitude between both coasts is due to friction with the bottom and lateral diffusion. Although an increase in the coefficients of friction against the bottom and lateral diffusion might result in a better fit between the results of the model and observation, it is clear that some other process not considered in this simplified model might be contributing to the difference of amplitudes observed between the two coasts.

In Fig. 14b the phases of the model can be seen to increase toward the head and then toward the mouth on the coast of Baja California if viewed from the mouth and on the mainland side. The behavior of the phases of the model is then similar to observations; for example, the difference of phase between La Paz and Topolobampo is 33 days according to the observations and 26 days according to the model; the difference between Loreto and Yávaros is 25 days in the observations and 17 days in the model; the difference between Guaymas and Santa Rosalía is 20 days in the observations and 12 days in the model.

4. Conclusions

The observations of sea level at the annual scale in the Gulf of California have been reproduced with a two-layer linear model. In the central and southern part of the gulf, the values of sea level elevation obtained with the model coincide quite well with observations, both in amplitude and phase, and to a lesser extent with the difference observed between the two coasts of the gulf. Near the head of the gulf, the model predicts amplitudes larger than those observed.

Three main forcing agents have been included: wind stress, surface heat flux, and the horizontal heat flux observed in the mouth of the gulf. We have assumed that the forcing in the mouth is due to the action of the Pacific Ocean, which forces an incoming baroclinic wave. The forcing agents produce mainly a baroclinic pattern of circulation. The wind stress also generates a barotropic circulation pattern restricted to shallow regions; however, the net offshore transport is almost null. Thus, the movement near the mouth is markedly baroclinic because in this region the topographic gradients are small and depths are large.

The amplitude of the horizontal heat flux in the mouth of the gulf has been fitted to 40 TW, which is the value observed by CLR94. The internal wave produces a horizontal heat flux of 33.8 TW, the wind stress 6.7 TW, and the surface heating 1.5 TW. The effect of each of these forcing agents on the variability observed in the elevation of sea level on the two coasts of the gulf is explained as follows: The internal wave produces an amplitude of sea level of 12 cm over the coasts of the gulf and the wind produces a slope in sea level varying from an almost null amplitude in the mouth to 8 cm in the head of the gulf; both forcing agents are responsible for the difference of phase between both coasts, the surface heating produces elevations of 1.25 cm that occur only in an area near the region of the islands, where this forcing agent is maximum. The difference of amplitude in sea level elevation between both coasts calculated with the model is caused by dissipative phenomena, that is, friction against the bottom and lateral diffusion.

The dynamics proposed here reproduce the horizontal distribution of horizontal heat flux in the interior of the gulf both in amplitude and phase. The results of the simulations show that variability across the gulf is as important as longitudinal variability for the two main forcing agents, wind stress and mouth's boundary condition. We attribute this to the small value of the internal radius of deformation in relation to the width of the gulf. Since we do not have sea level observations in the middle of the gulf, we cannot corroborate the important variability across the gulf predicted by the model.

The internal wave forced at the mouth and the wind

stress are in phase and produce the same pattern of circulation. Moreover, total circulation can be explained by means of an internal wave trapped against the wall that propagates around the coast of the gulf. The baroclinic wave is caused by the action of both the Pacific Ocean and the wind, which produces a forced internal wave. The internal wave propagates as a Kelvin-like signal, although very distorted by topography and friction against the bottom. However, individual effects of each forcing agent on coastal surface elevation and interface displacement are different. While the elevations of sea level produced by the internal wave are almost uniform in all the gulf, the wind produces elevations on the coast that grow linearly toward the head of the gulf.

The pattern of circulation obtained is cyclonic in summer and anticyclonic in winter. This pattern can be explained as an incoming flux and an outgoing flux intensified on the coasts of the gulf, which reverse their circulation direction from summer to winter. The surface layer is energetic and in the bottom layer velocities are low. The velocities of the upper layer reach maximum values of 70 cm s^{-1}. This is related to the depth of the upper layer, which has been chosen as $H_1 = 70$ m. Also, high velocities are related to large oscillations of the interface, which occur where the thickness of the lower layer vanishes. This might imply a large horizontal excursion of the interface in regions where it intercepts the topography. A future model should include the entrainment process that would prevent the interface from surfacing, cool the upper layer, and provide stress at the bottom of the upper layer.

Acknowledgments. This paper would not have been possible without Dr. Pedro Ripa's assistance and corrections. Adriana Usabiaga (UABC) was very helpful with language corrections. Dr. Miguel Lavín was very helpful with corrections of the manuscript. This work has been supported by CICESE's normal funding and by CONACyT (Mexico) under Grant 1282-T9204. Graduate scholarships were awarded by CICESE and CONACyT.

REFERENCES

Bennett, A. F., and P. C. McIntosh, 1982: Open ocean modeling as an inverse problem: Tidal theory. *J. Phys. Oceanogr.,* **12,** 1004–1018.

Bray, N. A., 1988: Thermohaline circulation in the Gulf of California. *J. Geophys. Res.,* **93,** 4993–5020.

Castro, R., M. F. Lavín, and P. Ripa, 1994: Seasonal heat balance in the Gulf of California. *J. Geophys. Res.,* **99,** 3249–3261.

Cushman-Roisin, B., and J. J. O'Brien, 1983: The influence of bottom topography on baroclinic transports. *J. Phys. Oceanogr.,* **13,** 1600–1611.

Gill, A., 1982: *Atmosphere–Ocean Dynamics.* Academic Press, 1662 pp.

Merrifield, M., 1992: A comparison of long coastal-trapped wave theory with remote-storm-generated wave events in the Gulf of California. *J. Phys. Oceanogr.,* **22,** 5–18.

——, and C. Winant, 1989: Shelf circulation in the Gulf of California: A description of the variability. *J. Geophys. Res.,* **94,** 18 133–18 160.

Ripa, P., 1990: Seasonal circulation in the Gulf of California. *Ann. Geophys.,* **8,** 559–564.

——, 1993: Conservation laws for primitive equations models with inhomogeneous layers. *Geophys. Astrophys. Fluid Dyn.,* **70,** 85–111.

——, 1997: Toward a physical explanation of the seasonal dynamics and thermodynamics of the Gulf of California. *J. Phys. Oceanogr.,* **27,** 597–614.

——, and S. G. Marinone, 1989: Seasonal variability of temperature, salinity, velocity, vorticity, and sea level in the central Gulf of California, as inferred from historical data. *Quart. J. Roy. Meteor. Soc.,* **115,** 887–913.

Taylor, G. I., 1921: Tidal oscillations in gulfs and rectangular basins. *Proc. London Math. Soc.,* **20,** 148–181.